Desalination and Water Treatment
www.deswater.com
doi: 10.5004/dwt.2018.22084

109 (2018) 176–187
March

Polymeric composite materials based on silicate: II. Sorption and distribution studies of some hazardous metals on irradiated doped polyacrylamide acrylic acid

M.M. Abou-Mesalam[a], M.R. Abass[a,*], M.A. Abdel-Wahab[a], E.S. Zakaria[a], A.M. Hassan[b]

[a]*Atomic Energy Authority, Hot Laboratories Centre, Post Code 13759, Cairo, Egypt, Tel. +20 1153334821, +20 1013439359; emails: mohamed.ragab@eaea.org.eg, mohamed.ragab201400@yahoo.com (M.R. Abass), mabumesalam@yahoo.com (M.M. Abou-Mesalam), drmagdameky1960@yahoo.com (M.A. Abdel-Wahab), essamzakareya@yahoo.com (E.S. Zakaria)*

[b]*Faculty of Science, Al-Azhar University, Cairo, Egypt, email: alihassanuk@yahoo.co.uk*

Received 4 October 2017; Accepted 19 February 2018

ABSTRACT

Magneso-silicate (MgSi) and polyacrylamide acrylic acid (Pam-Aa-MgSi) impregnated with magneso-silicate, as hybrid ion-exchange materials have chemical stability comparing with other composites ion-exchange materials. The capacities of MgSi, (Pam-Aa) and (Pam-Aa-MgSi) composites prepared at different radiation doses to Ni^{2+}, Cd^{2+}, Co^{2+}, Pb^{2+}, Zn^{2+} and Cu^{2+} ions were studied and the data indicated that their values of (Pam-Aa) and (Pam-Aa-MgSi) composites are lower than the values obtained for MgSi by 0.6 and 0.93 values, respectively. Distribution coefficients in nitric acid medium have been evaluated to explore the separation potentiality of MgSi, (Pam-Aa) and (Pam-Aa-MgSi) composites for mentioned cations. The data indicated that Cd^{2+} ion has high separation factor by 2.57, 2.13, 1.95, 1.93 and 1.42 for Pb^{2+}, Zn^{2+}, Co^{2+}, Cu^{2+} and Ni^{2+} ions, respectively, on MgSi and the selectivity for the investigated ions had the sequence: $Cd^{2+} > Ni^{2+} > Cu^{2+} \approx Co^{2+} \geq Zn^{2+} \geq Pb^{2+}$ on MgSi.

Keywords: Magneso-silicate; Chemical stability; Capacity; Distribution coefficients; Separation factor

1. Introduction

The most treacherous of the pollutants are heavy toxic metals, or a trace element such as lead, chromium, mercury, cadmium, nickel, iron, arsenic and cobalt. These toxic metals are non-biodegradable and can risk the human health by being accumulated in the food chain [1,2]. These toxic heavy metals are very dangerous to health, for example, lead is considered as a highly toxic element, when ingested or inhaled and adsorbed, it can harm virtually every system in the human body, especially brain, kidney and reproductive systems of both male and females. Lead harms many body systems because it disrupts enzyme systems mediated by other metals important to the body such as; iron, calcium and zinc [3]. Public concern over heavy metal pollution has demanded treatment of such effluents before disposal to the environment. Several techniques have been developed for the removal of such metal ions. These techniques include chemical precipitation, physical treatment such as ion-exchange, solvent extraction, reverse osmosis and adsorption [2,4]. Are the most widely used techniques for the removal of heavy toxic metals from wastewater streams. However, among all these methods, ion-exchange is one of the most attractive, cost effective, simple and widely used techniques for the treatment of wastewater containing heavy metals [5]. Nowadays, inorganic ion-exchange materials can use in analytical chemistry, owing to their thermal and radiation resistance as well as their chemical attack [6]. Organic polymers

* Corresponding author.

as ion exchangers are well known for their uniformity, chemical stability and control of their ion-exchange properties through synthetic methods [7,8]. To obtain a combination of these advantages associated with polymeric and inorganic materials as ion exchangers, attempts have been made to develop polymeric–inorganic composite ion exchangers by incorporation of organic monomers in the inorganic matrix. These materials were found selective for some toxic heavy metal ions and can utilized for the treatment of water pollution [3,9], environmental remediation [10,11], water softening [11], hydrometallurgy [11], catalysis [12], biochemistry [13] and selective adsorption [14,15] to medical applications [16–20]. Different inorganic ion-exchange materials based on silicate salts and polyacrylamide acrylic acid silicon titanate were synthesized earlier by Abou-Mesalam et al. [13,21] and used for removal of some heavy metals from industrial and hazardous wastes.

In this work magneso-silicate (MgSi), polyacrylamide acrylic acid (Pam-Aa) and polyacrylamide acrylic acid magneso-silicate (Pam-Aa-MgSi) composites prepared at radiation doses 25, 65 and 90 kGy were investigated for ion-exchange capacity, distribution coefficient and separation factor of chemically stable for Ni^{2+}, Cd^{2+}, Co^{2+}, Pb^{2+}, Zn^{2+} and Cu^{2+} ions.

2. Experimental

MgSi, (Pam-Aa) and (Pam-Aa-MgSi) materials were prepared as described earlier by Abou-Mesalam et al. [6,13,21].

2.1. Chemical stability

The chemical stability of MgSi, (Pam-Aa) and (Pam-Aa-MgSi) composites prepared at different radiation doses was studied in water and acid media (HNO_3 and HCl) in concentration range [10^{-3} to 6 M] by mixing 100 mg of each of the prepared samples and 100 mL of the desired solution with intermittent shaking for about 1 week at 25°C ± 1°C. The filtrate was tested gravimetrically [22].

2.2. Equilibrium time

All the measurements of equilibrium were done by shaking 0.2 g of MgSi, (Pam-Aa) and (Pam-Aa-MgSi) composites prepared at different radiation doses with 10 mL of Ni^{2+}, Cd^{2+}, Co^{2+}, Pb^{2+}, Zn^{2+} and Cu^{2+} ion solutions in a shaker thermostat at 25°C ± 1°C with V/m = 50 mL/g. After each time interval, the shaker is stopped and the solution is separated at once from the solid. The filtrate was taken to analyze for the determination of the concentration of the metal ions by atomic absorption spectrometer (AAS) model AA-6701 F-Shimadzu, Kyoto "Japan". The percentage uptake can be calculated by using the following equation [23]:

$$\%\text{ uptake} = \frac{C_i - C_f}{C_i} \times 100 \tag{1}$$

where C_i and C_f the initial and final concentration of metal ions in solution, respectively.

2.3. Effect of batch factor (V/m)

Batch factor was optimized by shaking different weights of composites with different volume of Ni^{2+}, Cd^{2+}, Co^{2+}, Pb^{2+}, Zn^{2+} and Cu^{2+} ion solutions (100 ppm) to obtain varying V/m ratios (V/m = 25, 50, 100, 200 and 400 mL/g). After an equilibrium, the solutions were separated and the filtrate was taken to analyze for the determination of the concentration of the metal ions by AAS. The percentage uptake can be calculated by using Eq. (1).

2.4. Capacity measurements

The capacities of MgSi, (Pam-Aa) and (Pam-Aa-MgSi) composites prepared at different radiation doses were determined using batch technique by repeated equilibrium of the composites with Ni^{2+}, Cd^{2+}, Co^{2+}, Pb^{2+}, Zn^{2+} and Cu^{2+} ion solutions. 1 g of each solid material was equilibrated with 50 mL of 100 ppm Ni^{2+}, Cd^{2+}, Co^{2+}, Pb^{2+}, Zn^{2+} and/or Cu^{2+} ion solutions by V/m = 50 mL/g. The mixture was shaken for 1 day at 25°C ± 1°C. After equilibrium, the liquid phase was separated by centrifugation and replaced by the same volume of the initial solution. The procedure was repeated until no further absorption of cations occurred. The capacity was calculated from the following equation [2,11]:

$$\text{Capacity} = \text{uptake} \bullet C_0 \bullet \frac{V}{m}\,\text{mg/g} \tag{2}$$

where C_o is the initial concentration of solution, mg/L; V is the solution volume, mL and m is the weight of the composite, g.

2.5. Effect of [H+] ion on distribution studies

The distribution coefficient (K_d) values on MgSi, (Pam-Aa) and (Pam-Aa-MgSi) composites prepared at different radiation doses as a function of different concentration of H^+ ion was investigated using batch technique. 0.2 g of composites were shaken at 25°C ± 1°C with 10 mL of Ni^{2+}, Cd^{2+}, Co^{2+}, Pb^{2+}, Zn^{2+} and Cu^{2+} ion solutions (100 mg/L) with a V/m ratio of 50 mL/g. The [H^+] concentrations were adjusted to 10^{-3}, 10^{-2}, 10^{-1}, 0.5, 1, 2 and 4 M. After an overnight standing (sufficient to attain the equilibrium), the solution is separated at once from the solid and the filtrate was taken to analyze for the determination of the concentration of metal ions by AAS. The distribution coefficient (K_d) and separation factor ($\alpha^A{}_B$) values were calculated using the following equations [2,4,6]:

$$K_d = \frac{(A_0 - A_{\text{eq.}})}{A_{\text{eq.}}}\, x \frac{V}{m}\,\text{ml/g} \tag{3}$$

$$\text{Separation factor } (\alpha^{A}{}_{B}) = \frac{K_d(B)}{K_d(A)} \tag{4}$$

where A_o and A_{eq} are the concentrations of the ions in solutions before and after equilibration, respectively, V is the solution volume, m is the composite weight and $K_d(A)$ and $K_d(B)$ are the distribution coefficients for the two competing species A and B in the system.

3. Results and discussion

The scope of this work is the attempt to study capacity and sorption investigation of a high chemical stable inorganic, organic and composite ion-exchange materials MgSi, (Pam-Aa) and (Pam-Aa-MgSi) composites prepared at different radiation doses.

The chemical stability of MgSi, (Pam-Aa) and (Pam-Aa-MgSi) composites prepared at different radiation doses was studied in water, nitric acid and hydrochloric acid media and the data are shown in Table 1. From this table, we find that MgSi, (Pam-Aa) and (Pam-Aa-MgSi) composites prepared at different radiation doses are stable in H_2O, nitric acid and hydrochloric acid up to 6 M, and partially dissolved in acid media higher than 6 M. The solubility values were increased with the increasing of the acid concentration. The chemical stability of the prepared MgSi in acid medium is agree with the chemical stability of with SiTi [22] (Pam-Aa) and (Pam-Aa-MgSi) composites are more stable than polypyrrole Th(IV) phosphate [9], especially at high acid concentration (4 M HCl and 4 M HNO_3), polyaniline Sn(IV) tungstoarsenate [24], especially at de mineralize water and high acid concentration (4 M HCl and 4 M HNO_3), poly(acrylamide-acrylic acid)-silicon titanate [21] and polypyrrole/polyantimonic acid [21], while polyaniline Sn(IV) phosphate [25], is more chemically stable than the prepared (Pam-Aa) and (Pam-Aa-MgSi) composites. Also, the data indicates that MgSi composite has a higher stability than (Pam-Aa) and (Pam-Aa-MgSi) composites prepared at different radiation doses, this may be due to the higher crystallinity of magneso-silicate composite to polymer composites as mention earlier in X-Ray diffraction pattern studies [26], and also may be due to the higher water content of polymer composites compared with magneso-silicate composite. And from the data obtained, it is clear that the solubility decreased with the increasing of radiation doses, this may be due to increasing of crosslinking in the polymers, where the crosslinking increase by increasing radiation dose. And also from the results obtain in Table 1, it is clear that (Pam-Aa-MgSi) composites have higher chemical stability than (Pam-Aa) copolymers, this may be due to the higher crystallinity and complexation of (Pam-Aa-MgSi) composites than (Pam-Aa) copolymers.

The variation of adsorption percentage of Ni^{2+}, Cd^{2+}, Co^{2+}, Pb^{2+}, Zn^{2+} and Cu^{2+} ions onto MgSi, (Pam-Aa) and (Pam-Aa-MgSi) composites with shaking time was carried out as shown in Figs. 1(a)–(c), respectively. It is seen that the percentage uptake increases with the increase in shaking time and maximum adsorption was observed at 24 h on all prepared composites. Therefore, we can consider these times are sufficient to attain equilibrium for Ni^{2+}, Cd^{2+}, Co^{2+}, Pb^{2+}, Zn^{2+} and/or Cu^{2+} ions onto MgSi, (Pam-Aa) and (Pam-Aa-MgSi) composites and used for all further experiments.

Effect of batch factor (the ratio of volume solution (V) to the amount of exchanger (m)) on the percentage uptake of Ni^{2+}, Cd^{2+}, Co^{2+}, Pb^{2+}, Zn^{2+} and/or Cu^{2+} ion solutions (100 ppm) by MgSi, (Pam-Aa) and (Pam-Aa-MgSi) ion exchangers was studied. Optimization was carried out by shaking 10 mL of solutions containing Ni^{2+}, Cd^{2+}, Co^{2+}, Pb^{2+}, Zn^{2+} and/or Cu^{2+} ion solutions (100 ppm) for 24 h with various amounts (0.025, 0.05, 0.1, 0.2 or 0.4 g) of ion exchangers. The ratios of V/m were 25, 50, 100, 200 and 400. The results are given in

Table 1
Chemical stability of MgSi, (Pam-Aa) and (Pam-Aa-MgSi) composites prepared at different radiation doses in different media at 25°C ± 1°C

Sample	Radiation dose	Solubility (g/L at 25°C ± 1°C)														
		H_2O	HNO_3 (M)							HCl (M)						
			10^{-3}	10^{-2}	10^{-1}	0.5	1	3	6	10^{-3}	10^{-2}	10^{-1}	0.5	1	3	6
MgSi	–	B.D.L.	0.0032	0.061	0.12	0.21	0.29	0.32	0.65	0.0022	0.059	0.11	0.22	0.32	0.45	0.66
(Pam-Aa)	25 kGy	B.D.L.	0.0056	0.086	0.25	0.35	0.46	0.49	0.77	0.0042	0.066	0.18	0.29	0.44	0.56	0.77
	65 kGy	B.D.L.	0.0051	0.076	0.22	0.31	0.41	0.46	0.72	0.0039	0.062	0.17	0.25	0.42	0.52	0.75
	90 kGy	B.D.L.	0.0035	0.071	0.18	0.24	0.33	0.41	0.69	0.0035	0.061	0.13	0.23	0.39	0.5	0.71
(Pam-Aa-MgSi)	25 kGy	B.D.L.	0.0038	0.072	0.22	0.32	0.43	0.52	0.69	0.0046	0.066	0.16	0.25	0.39	0.49	0.74
	65 kGy	B.D.L.	0.0034	0.071	0.17	0.26	0.36	0.44	0.65	0.0043	0.064	0.12	0.24	0.35	0.46	0.71
	90 kGy	B.D.L.	0.0031	0.062	0.12	0.22	0.32	0.42	0.61	0.0033	0.061	0.11	0.21	0.33	0.44	0.65

B.D.L., Below detection limit.

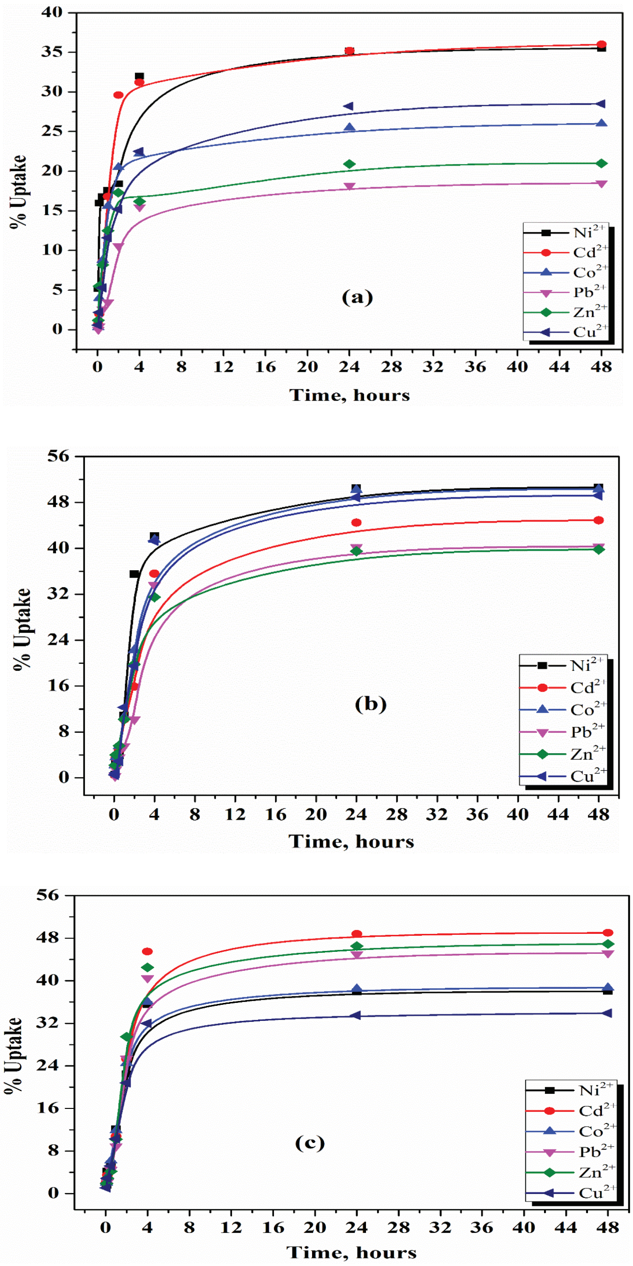

Fig. 1. Effect of contact time on percentage uptake of Ni^{2+}, Cd^{2+}, Co^{2+}, Pb^{2+}, Zn^{2+} and Cu^{2+} ions on MgSi (a), (Pam-Aa) (b) and (Pam-Aa-MgSi) (c) composites at 25°C ± 1°C.

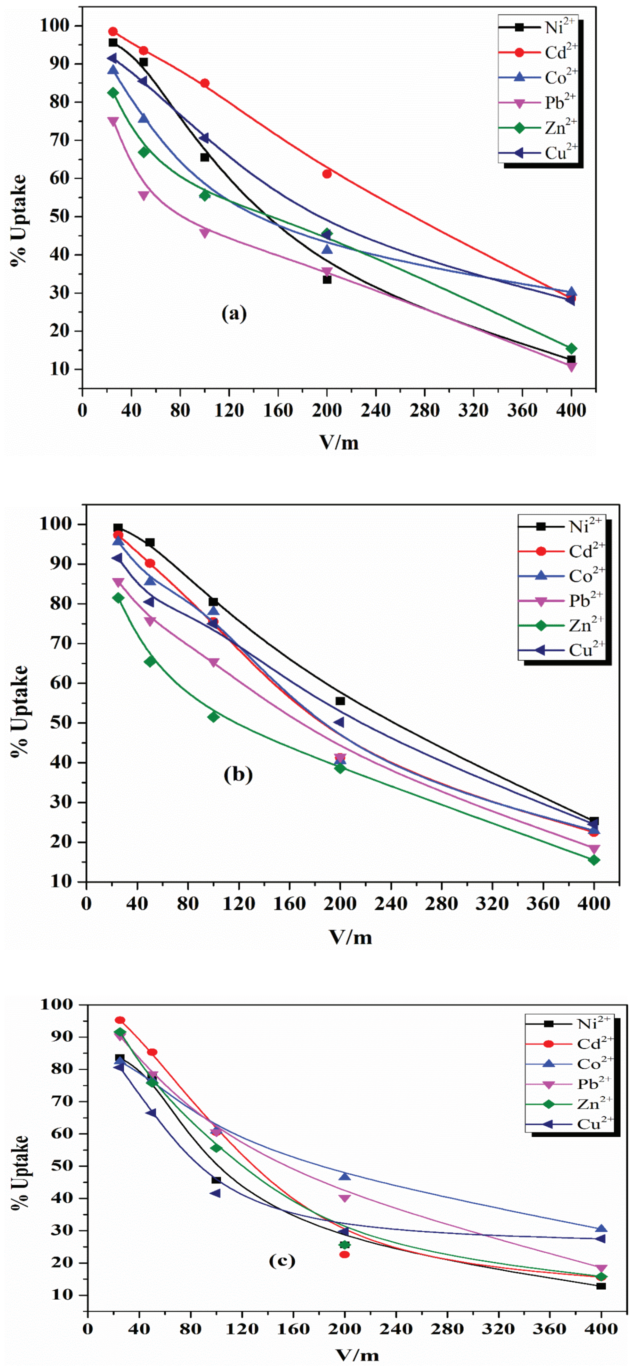

Fig. 2. Effect of V/m on percentage uptake of Ni^{2+}, Cd^{2+}, Co^{2+}, Pb^{2+}, Zn^{2+} and Cu^{2+} ions on MgSi (a), (Pam-Aa) (b) and (Pam-Aa-MgSi) (c) composites at 25°C ± 1°C.

Figs. 2(a)–(c). From this figure, it is clear that retention of Ni^{2+}, Cd^{2+}, Co^{2+}, Pb^{2+}, Zn^{2+} and/or Cu^{2+} ions on the MgSi, (Pam-Aa) and (Pam-Aa-MgSi) composites decrease with increasing the (V/m) ratio and the ratio (25) is the best ratio for maximum retention value.

The ion-exchange capacities of MgSi, (Pam-Aa) and (Pam-Aa-MgSi) composites prepared at different radiation doses for Ni^{2+}, Cd^{2+}, Co^{2+}, Pb^{2+}, Zn^{2+} and/or Cu^{2+} ions were determined at 25°C ± 1°C. The data are tabulated in Table 2. Table 2 indicates that the affinity sequence for all cations is: $Cu^{2+} > Ni^{2+} \approx Co^{2+} > Pb^{2+} \geq Zn^{2+} > Cd^{2+}$ for MgSi. This sequence is in accordance with the unhydrated radii of the exchanging ions, whereas the ions with smaller unhydrated radii easily enter the pores of the exchanger, resulting in higher adsorption [7,27–29]. The high capacity of MgSi for cupper ion may be due to the higher complexing ability of cupper with the presence in more than one oxidation states. The lower capacity of magneso-silicate for Cd^{2+} ion reflects the non-selectivity of MgSi for Cd^{2+} ion.

Also, the data in Table 2 show that the ion-exchange capacities of (Pam-Aa) and (Pam-Aa-MgSi) composites

Table 2
Capacity values of various exchanging ions onto MgSi, (Pam-Aa) and (Pam-Aa-MgSi) composites prepared at different radiation doses at 25°C ± 1°C

Exchanging ions	Ionic radii (Å)	Hydration energy	MgSi	
			Capacity (mg/g)	Metal exchange
Ni^{2+}	0.72	2,054	12.1	Unhydrated
Cd^{2+}	0.97	1,806	1.35	Unhydrated
Co^{2+}	0.72	2,054	12.0	Unhydrated
Pb^{2+}	1.20	1,480	4.8	Unhydrated
Zn^{2+}	0.74	2,044	4.5	Hydrated
Cu^{2+}	0.72	2,100	15.2	Unhydrated

Exchanging ions	Ionic radii (Å)	Hydration energy	(Pam-Aa) at radiation dose 25 kGy		(Pam-Aa) at radiation dose 65 kGy		(Pam-Aa) at radiation dose 90 kGy	
			Capacity (mg/g)	Metal exchange	Capacity (mg/g)	Metal exchange	Capacity (mg/g)	Metal exchange
Ni^{2+}	0.72	2,054	11.2	Unhydrated	11.2	Unhydrated	11.1	Unhydrated
Cd^{2+}	0.97	1,806	1.0	Unhydrated	1.0	Unhydrated	1.12	Unhydrated
Co^{2+}	0.72	2,054	12.0	Unhydrated	12.4	Unhydrated	12.0	Unhydrated
Pb^{2+}	1.20	1,480	3.0	Unhydrated	3.7	Unhydrated	3.3	Unhydrated
Zn^{2+}	0.74	2,044	2.3	Hydrated	2.7	Hydrated	2.7	Hydrated
Cu^{2+}	0.72	2,100	0.18	Hydrated	0.25	Hydrated	0.24	Hydrated

Exchanging ions	Ionic radii (Å)	Hydration energy	(Pam-Aa-MgSi) at radiation dose 25 kGy		(Pam-Aa-MgSi) at radiation dose 65 kGy		(Pam-Aa-MgSi) at radiation dose 90 kGy	
			Capacity (mg/g)	Metal exchange	Capacity (mg/g)	Metal exchange	Capacity (mg/g)	Metal exchange
Ni^{2+}	0.72	2,054	11.5	Unhydrated	11.7	Unhydrated	11.9	Unhydrated
Cd^{2+}	0.97	1,806	2.54	Unhydrated	3.1	Unhydrated	2.6	Unhydrated
Co^{2+}	0.72	2,054	12.0	Unhydrated	12.1	Unhydrated	12.0	Unhydrated
Pb^{2+}	1.20	1,480	5.2	Unhydrated	5.3	Unhydrated	5.3	Unhydrated
Zn^{2+}	0.74	2,044	5.8	Hydrated	7.1	Hydrated	7.4	Hydrated
Cu^{2+}	0.72	2,100	6.2	Hydrated	8.9	Hydrated	8.2	Hydrated

prepared at different radiation doses for mentioned cations is lower than that obtained for MgSi by 0.6 and 0.93 values, respectively, with the sequence order: $Co^{2+} \geq Ni^{2+} > Pb^{2+} > Zn^{2+} > Cd^{2+} > Cu^{2+}$ and $Co^{2+} \geq Ni^{2+} > Cu^{2+} > Zn^{2+} > Pb^{2+} > Cd^{2+}$ for (Pam-Aa) and (Pam-Aa-MgSi), respectively. These results suggest that the composites keeping cavity for exchangeable ions in the framework by polymer composites of these cations with MgSi [6]. The high capacity of (Pam-Aa) for cobalt ion may be due to the higher complexing ability of cobalt with the presence in more than one oxidation states [16]. The lower capacity of (Pam-Aa) for Cu^{2+} ion reflects the non-selectivity of (Pam-Aa) for Cu^{2+} ion. Also, the lower capacity of (Pam-Aa-MgSi) for Cd^{2+} and Pb^{2+} ions reflects the non-selectivity of (Pam-Aa-MgSi) for Cd^{2+} and Pb^{2+} ions. Also, the data in Table 2 shows a relatively high capacity of (Pam-Aa-MgSi) compared with (Pam-Aa) for the studied cations that may be due to the impregnation of MgSi to (Pam-Aa) material increases the number of acidic sites on the surface of (Pam-Aa-MgSi) [16].

The distribution coefficients (K_d; mL/g) and separation factors (α) of Ni^{2+}, Cd^{2+}, Co^{2+}, Pb^{2+}, Zn^{2+} and/or Cu^{2+} ions onto MgSi, (Pam-Aa) and (Pam-Aa-MgSi) composites prepared at different radiation doses of the range (10^{-3} to 4 M) HNO_3 medium were calculated and tabulated in Tables 3–5 and shown in Fig. 3. The preliminary studies indicate that, the time of equilibrium for mentioned cations onto prepared ion-exchange materials was attained after 24 h (sufficient to attain equilibrium) in a shaker thermostat adjusted at 25°C ± 1°C.

The data in Fig. 3 show that K_d values are inversely proportional to the $[H^+]$ ion concentration of the media. This is an obvious phenomenon where, by increase of the $[H^+]$ ion of the medium, the chance of the replacement of metal ions Ni^{2+}, Cd^{2+}, Co^{2+}, Pb^{2+}, Zn^{2+} and/or Cu^{2+} with H^+ ion in the composite decreased that lead to decrease of percentage uptake of these cations onto the composites [30].

Fig. 3(a) and Table 3 show the $[H^+]$ dependency of K_d values of Ni^{2+}, Cd^{2+}, Co^{2+}, Pb^{2+}, $Zn^{2+}$and/or Cu^{2+} ions onto MgSi. On the other hand, the linear relations between $\log K_d$ and $[H^+]$ were observed for Ni^{2+}, Cd^{2+}, Co^{2+}, Pb^{2+}, Zn^{2+} and/or Cu^{2+} ions with slopes 0.28, 0.31, 0.25, 0.32, 0.37 and 0.13, respectively. These slopes did not equal to the valence of the metal ions sorbed, which prove the non-ideality of the exchange reaction. The variation may be due to the prominence of a mechanism other than ion-exchange, such as precipitation, surface adsorption or simultaneous adsorption of anions [6,7].

The distribution coefficients (K_d) and separation factors (α) for the mentioned cations in 10^{-3} M HNO_3 medium were calculated and tabulated in Table 3. The data in Table 3 indicate that the distribution coefficients have the affinity sequence: $Cd^{2+} > Ni^{2+} > Cu^{2+} \approx Co^{2+} \geq Zn^{2+} \geq Pb^{2+}$.

For MgSi, this sequence supported that the sorption of metal ions was carried out in unhydrated ionic radii except Cd^{2+} ion adsorbed as hydrated ionic radii. The ions with smaller unhydrated ionic radii easily enter the cavities of the exchanger resulting in a higher uptake and hence K_d increases [29]. The separation factors for the studied cations were calculated and indicated that, Cd^{2+} ion has a higher separation factor by 2.57, 2.13, 1.95, 1.93 and 1.42 for Pb^{2+}, Zn^{2+}, Co^{2+}, Cu^{2+} and Ni^{2+} ions, respectively, these values indicated that Cd^{2+} ion can easily separate from radioactive and industrial

Table 3
K_d values and separation factors (α) for Ni^{2+}, Cd^{2+}, Co^{2+}, Pb^{2+}, Zn^{2+} and/or Cu^{2+} ions onto MgSi at 25°C ± 1°C

$[H^+]$	K_d (mL/g) and (α)	Pb^{2+}	Zn^{2+}	Co^{2+}	Cu^{2+}	Ni^{2+}	Cd^{2+}
10^{-3}	K_d (α)	49.1	59.2	64.6	65.3	88.6	126
			1.21	1.32	1.33	1.8	2.57
				1.09	1.1	1.5	2.13
					1.01	1.37	1.95
						1.36	1.93
							1.42
10^{-2}	K_d (α)	39.9	55.2	57	57.1	78.9	123
			1.38	1.43	1.43	1.98	3.08
				1.03	1.03	1.43	2.23
					1	1.38	2.16
						1.38	2.15
							1.56
10^{-1}	K_d (α)	32.8	41.8	53.9	53.7	76.4	110
			1.27	1.64	1.64	2.33	3.35
				1.29	1.28	1.83	2.63
					1	1.42	2.04
						1.42	2.04
							1.44
0.5	K_d (α)	24.9	35.1	49.7	49.1	65.9	80.5
			1.41	2	1.97	2.65	3.23
				1.42	1.4	1.88	2.29
					0.99	1.33	1.62
						1.34	1.64
							1.22
1	K_d (α)	22.9	19	33.1	44.4	48.1	51
			0.83	1.45	1.94	2.1	2.23
				1.74	2.34	2.53	2.68
					1.34	1.45	1.54
						1.08	1.15
							1.06
2	K_d (α)	14.7	11.4	12.9	35.3	26.8	20.8
			0.78	0.88	2.4	1.82	1.41
				1.13	3.1	2.35	1.82
					2.74	2.08	1.61
						0.76	0.59
							0.78
4	K_d (α)	1.8	1.6	6.6	16	6.2	7.4
			0.89	3.67	8.89	3.44	4.11
				4.13	10	3.88	4.63
					2.42	0.94	1.12
						0.39	0.46
							1.19

Table 4
K_d values and separation factors (α) for Ni^{2+}, Cd^{2+}, Co^{2+}, Pb^{2+}, Zn^{2+} and/or Cu^{2+} ions onto (Pam-Aa) at different radiation dose at 25°C ± 1°C

$[H^+]$	K_d (mL/g) and (α)	(Pam-Aa) at radiation dose 25 kGy						(Pam-Aa) at radiation dose 65 kGy						(Pam-Aa) at radiation dose 90 kGy					
		Zn^{2+}	Pb^{2+}	Cu^{2+}	Co^{2+}	Cd^{2+}	Ni^{2+}	Pb^{2+}	Zn^{2+}	Co^{2+}	Cu^{2+}	Cd^{2+}	Ni^{2+}	Zn^{2+}	Pb^{2+}	Cu^{2+}	Cd^{2+}	Ni^{2+}	Co^{2+}
10^{-3}	$K_d(\alpha)$	28.5	49.8	55.6	97.7	110	130	38.6	45.7	51.4	58.6	113	115	48	59.1	76.7	120	123	211
			1.75	1.95	3.43	3.86	4.56		1.18	1.33	1.52	2.93	2.98		1.23	1.6	2.5	2.56	4.4
				1.12	1.96	2.21	2.61			1.12	1.28	2.47	2.52			1.3	2.03	2.08	3.57
					1.76	1.98	2.34				1.14	2.2	2.24				1.56	1.6	2.75
						1.13	1.33					1.93	1.96					1.02	1.76
							1.18						1.02						1.72
10^{-2}	$K_d(\alpha)$	26.2	37.3	52.1	86.7	107	107	35.4	41.9	48.1	51.8	109	114	45.3	57.6	74.7	118	121	200
			1.42	1.99	3.31	4.08	4.08		1.18	1.36	1.46	3.08	3.22		1.27	1.65	2.6	2.67	4.42
				1.4	2.32	2.87	2.87			1.16	1.24	2.6	2.72			1.3	2.05	2.1	3.47
					1.66	2.05	2.05				1.08	2.27	2.37				1.58	1.62	2.68
						1.23	1.23					2.1	2.2					1.03	1.69
							1						1.05						1.65
10^{-1}	$K_d(\alpha)$	20.5	32.9	49.8	64.9	93	80.4	33.1	37.4	45.8	49.5	99.2	97.8	40.8	55.2	68.3	107	114	142
			1.6	2.43	3.17	4.54	3.92		1.13	1.38	1.5	3	2.95		1.35	1.67	2.62	2.79	3.48
				1.51	1.97	2.83	2.44			1.22	1.32	2.65	2.61			1.24	1.94	2.07	2.57
					1.3	1.87	1.61				1.08	2.17	2.14				1.57	1.67	2.08
						1.43	1.24					2	1.98					1.07	1.33
							0.86						0.99						1.24
0.5	$K_d(\alpha)$	14.3	23	47.3	54	89.5	53.2	22.5	30.8	44	47.9	90.4	64	31.4	33.1	49.7	80.4	63.1	63.2
			1.61	3.31	3.78	6.26	3.72		1.37	1.96	2.13	4.02	2.84		1.05	1.58	2.56	2.01	2.01
				2.06	2.35	3.89	2.31			1.43	1.56	2.94	2.08			1.5	2.43	1.91	1.91
					1.14	1.89	1.12				1.09	2.05	1.45				1.62	1.27	1.27
						1.65	0.99					1.89	1.34					0.78	0.79
							0.59						0.71						1
1	$K_d(\alpha)$	9.8	14.1	46.5	43.5	75.9	39.1	12.5	25.8	26.3	46.7	75.9	44.8	17.7	17.9	25.2	49.5	37.8	23
			1.44	4.74	4.44	7.74	3.99		2.06	2.1	3.74	6.07	3.58		1.01	1.42	2.8	2.14	1.3
				3.3	3.09	5.38	2.77			1.02	1.81	2.94	1.74			1.41	2.77	2.11	1.28
					0.94	1.63	0.84				1.78	2.89	1.7				1.96	1.5	0.91
						1.74	0.9					1.63	0.96					0.76	0.46
							0.52						0.59						0.61

(Continued)

Table 4 *(Continued)*

[H^+]	K_d (mL/g) and (α)	(Pam-Aa) at radiation dose 25 kGy						(Pam-Aa) at radiation dose 65 kGy						(Pam-Aa) at radiation dose 90 kGy					
		Zn^{2+}	Pb^{2+}	Cu^{2+}	Co^{2+}	Cd^{2+}	Ni^{2+}	Pb^{2+}	Zn^{2+}	Co^{2+}	Cu^{2+}	Cd^{2+}	Ni^{2+}	Zn^{2+}	Pb^{2+}	Cu^{2+}	Cd^{2+}	Ni^{2+}	Co^{2+}
2	K_d (α)	5.3	7.9	35.7	32.7	30.1	28.3	2.9	14.3	16.9	35.7	22.8	32	9.46	7.9	9.3	12.2	12.7	6.72
			1.49	6.74	6.17	5.68	5.34		4.93	5.83	12.3	7.86	11		0.85	0.98	1.29	1.34	0.71
				4.52	4.14	3.81	3.58			1.18	2.5	1.59	2.24			1.18	1.54	1.61	0.85
					0.92	0.84	0.79				2.11	1.35	1.89				1.31	1.37	0.72
						0.92	0.87					0.64	0.9					1.04	0.55
							0.94						1.4						0.53
4	K_d (α)	1.7	1.4	13.9	8.5	7.4	7.1	0.34	8.9	10.3	21.9	9.3	14.4	0.88	2.37	1.22	2.83	1.62	0.63
			0.82	8.18	5	4.35	4.18		26.2	30.3	64.41	27.4	42.4		2.69	1.39	3.22	1.84	0.72
				9.93	6.07	5.29	5.07			1.16	2.46	1.04	1.62			0.51	1.19	0.68	0.27
					0.61	0.53	0.51				2.13	0.9	1.4				2.32	1.33	0.52
						0.87	0.84					0.42	0.66					0.57	0.22
							0.96						1.55						0.39

Table 5
K_d values and separation factors (α) for Ni^{2+}, Cd^{2+}, Co^{2+}, Pb^{2+}, Zn^{2+} and/or Cu^{2+} ions onto (Pam-Aa-MgSi) at different radiation dose at 25°C ± 1°C

[H^+]	K_d (mL/g) and (α)	(Pam-Aa-MgSi) at radiation dose 25 kGy						(Pam-Aa-MgSi) at radiation dose 65 kGy						(Pam-Aa-MgSi) at radiation dose 90 kGy					
		Cu^{2+}	Co^{2+}	Ni^{2+}	Pb^{2+}	Zn^{2+}	Cd^{2+}	Cu^{2+}	Ni^{2+}	Zn^{2+}	Co^{2+}	Cd^{2+}	Pb^{2+}	Zn^{2+}	Cu^{2+}	Co^{2+}	Ni^{2+}	Cd^{2+}	Pb^{2+}
10^{-3}	K_d (α)	58.8	59.2	95.9	100	111	114	62.9	91.3	93.3	103	103	343	60.9	63.2	86.6	111	119	140
			1.01	1.63	1.7	1.89	1.94		1.45	1.48	1.64	1.64	5.45		1.04	1.42	1.82	1.95	2.3
				1.62	1.69	1.88	1.93			1.02	1.13	1.13	3.76			1.37	1.76	1.89	2.22
					1.04	1.16	1.19				1.1	1.1	3.68				1.28	1.37	1.62
						1.11	1.14					1	3.33					1.07	1.26
							1.03						3.33						1.18
10^{-2}	K_d (α)	55.6	57.3	91.3	99.8	107	107	60.4	88.6	80.4	102	98.1	334	60.8	62.1	85.4	94.4	101	126
			1.03	1.64	1.79	1.92	1.92		1.47	1.33	1.69	1.62	5.53		1.02	1.4	1.55	1.66	2.07
				1.59	1.74	1.87	1.87			0.91	1.15	1.11	3.77			1.38	1.52	1.63	2.03
					1.09	1.17	1.17				1.27	1.2	4.15				1.105	1.18	1.48
						1.07	1.07					0.96	3.27					1.07	1.33
							1						3.4						1.25

(Continued)

Table 5 (*Continued*)

$[H^+]$	K_d (mL/g) and (α)	(Pam-Aa-MgSi) at radiation dose 25 kGy						(Pam-Aa-MgSi) at radiation dose 65 kGy						(Pam-Aa-MgSi) at radiation dose 90 kGy					
		Cu^{2+}	Co^{2+}	Ni^{2+}	Pb^{2+}	Zn^{2+}	Cd^{2+}	Cu^{2+}	Ni^{2+}	Zn^{2+}	Co^{2+}	Cd^{2+}	Pb^{2+}	Zn^{2+}	Cu^{2+}	Co^{2+}	Ni^{2+}	Cd^{2+}	Pb^{2+}
10^{-1}	K_d (α)	53.9	54.9	87.4	84.1	74.2	103	58.5	81.4	58.5	90.4	91.5	256	57.7	60.4	82	85.7	96	106
			1.02	1.62	1.56	1.38	1.91		1.39	1	1.55	1.56	4.38		1.05	1.42	1.49	1.66	1.84
				1.59	1.53	1.35	1.88			0.72	1.11	1.12	3.14			1.36	1.42	1.59	1.75
					0.96	0.85	1.18				1.55	1.56	4.38				1.05	1.17	1.29
						0.88	1.22					1.01	2.83					1.12	1.24
							1.39						2.8						1.1
0.5	K_d (α)	47.7	42.3	63.2	25.4	43	86.1	43.8	61.8	30.8	63.2	65.4	95.4	30.8	39.8	57	48.6	46.2	68
			0.89	1.32	0.53	0.9	1.81		1.41	0.7	1.44	1.49	2.18		1.29	1.85	1.58	1.5	2.21
				1.49	0.6	1.02	2.04			0.5	1.02	1.06	1.54			1.43	1.22	1.16	1.71
					0.4	0.68	1.36				2.05	2.12	3.1				0.85	0.81	1.19
						1.69	3.38					1.03	1.51					0.95	1.4
							2						1.46						1.47
1	K_d (α)	36.8	33.7	49.6	14.5	16.3	57.9	31.6	43.3	10.1	33.1	41.8	25.8	15.9	23.7	45.5	16.8	16.8	35.1
			0.92	1.35	0.39	0.44	1.57		1.37	0.32	1.05	1.32	0.82		1.49	2.86	1.06	1.068	2.21
				1.47	0.43	0.48	1.72			0.23	0.76	0.97	0.6			1.92	0.71	0.71	1.48
					0.29	0.33	1.17				3.28	4.14	2.55				0.37	0.37	0.77
						1.12	3.99					1.26	0.78					1	2.1
							3.55						0.62						2.1
2	K_d (α)	24.1	21	33.7	2.6	3.29	26.3	16.9	21.6	1.44	14.5	15.7	3.18	3.81	6.42	26.6	5.71	6.66	9.69
			0.87	1.4	0.11	0.14	1.09		1.28	0.09	0.86	0.93	0.19		1.69	6.98	1.5	1.75	2.54
				1.6	0.12	0.16	1.25			0.07	0.67	0.73	0.15			4.14	0.89	1.04	1.51
					0.08	0.1	0.78				10.1	10.9	2.21				0.21	0.25	0.36
						1.27	10.1					1.08	0.22					1.17	1.7
							7.99						0.2						1.45
4	K_d (α)	10.7	6.6	17.9	0.08	0.16	7.14	4.34	5.44	0.05	1.5	2.09	0.08	0.16	0.3	8.53	0.09	1.14	0.94
			0.62	1.67	0.007	0.01	0.67		1.25	0.01	0.35	0.48	0.02		1.88	53.3	0.56	7.13	5.88
				2.71	0.01	0.02	1.08			0.009	0.28	0.38	0.01			28.4	0.3	3.8	3.13
					0.004	0.009	0.4				30	41.8	1.6				0.01	0.13	0.11
						2	89.3					1.39	0.05					12.7	10.4
							44.6						0.04						0.82

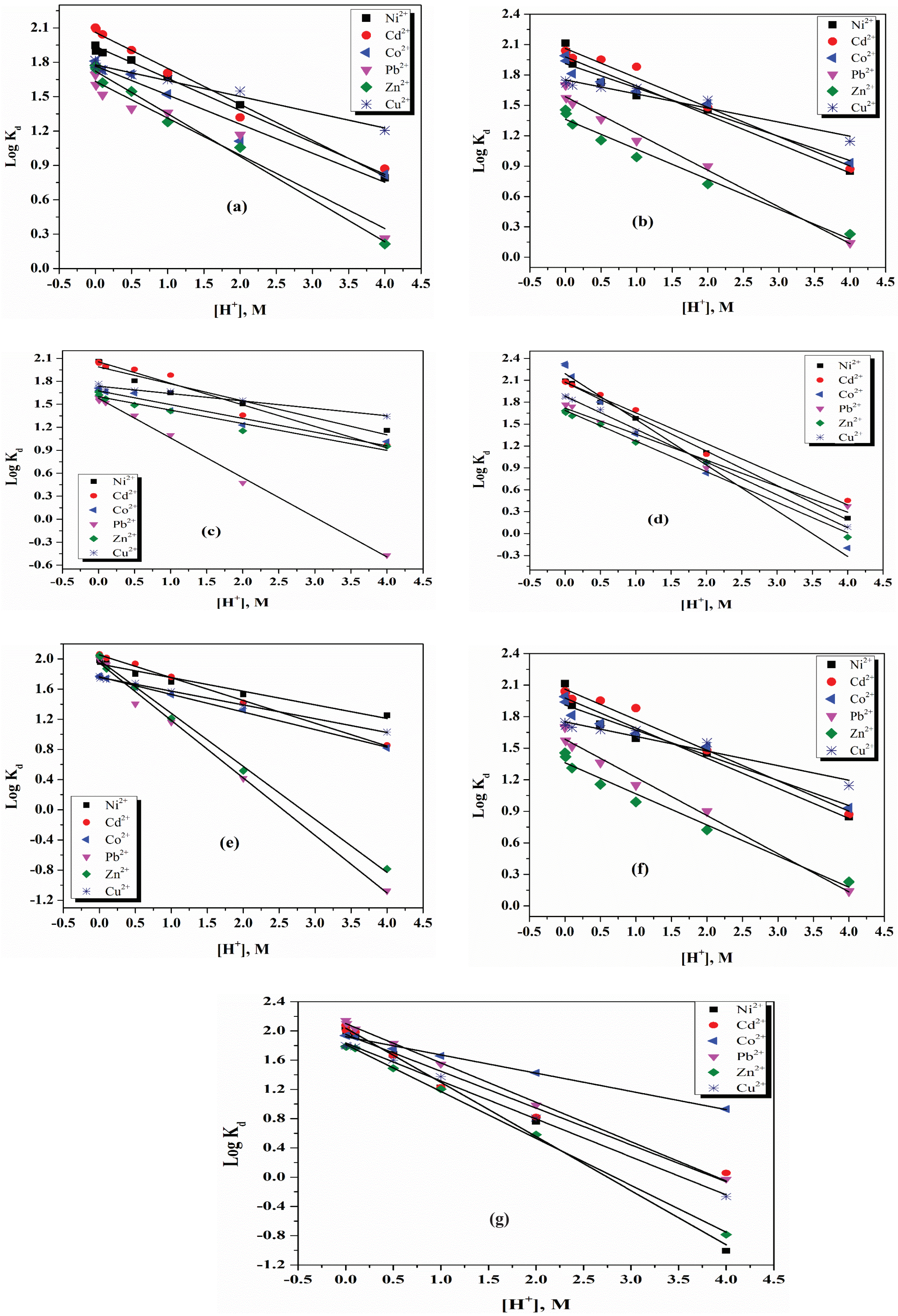

Fig. 3. Plots of logK_d against [H$^+$] ion of Ni^{2+}, Cd^{2+}, Co^{2+}, Pb^{2+}, Zn^{2+} and Cu^{2+} ions onto MgSi (a), (Pam-Aa) at radiation dose 25,65 and 90 kGy (b)–(d), respectively. And (Pam-Aa-MgSi) at radiation dose 25, 65 and 90 kGy (e)–(g), respectively at 25°C ± 1°C.

waste solutions included the abovementioned cations, and these values reflect that non-selectivity of MgSi for Pb^{2+} ion.

Figs. 3(b)–(d) and Table 4 show the $[H^+]$ dependency of K_d values of divalent metal cations Ni^{2+}, Cd^{2+}, Co^{2+}, Pb^{2+}, Zn^{2+} and/or Cu^{2+} ions onto (Pam-Aa) copolymers prepared at different radiation dose. Linear relations between $\log K_d$ and $[H^+]$ were observed for Ni^{2+}, Cd^{2+}, Co^{2+}, Pb^{2+}, Zn^{2+} and Cu^{2+} ions with slopes (0.28, 0.29, 0.24, 0.36, 0.3 and 0.13), (0.22, 0.28, 0.18, 0.52, 0.18 and 0.1) and (0.47, 0.42, 0.63, 0.36, 0.42 and 0.45) for (Pam-Aa) at radiation doses 25, 65 and 90 kGy, respectively. These slopes did not equal to the valence of the divalent metal sorbed, which prove that the deviation from ideality of the ion-exchange reaction for all studied metal ions on (Pam-Aa) at different radiation doses [29]. The non-ideality may be due to a different mechanism such as physical adsorption; in addition, this may be due to exchange ion replaced; some impurities presented in the matrix, and may be due to complexity of the system [6].

The distribution coefficients (K_d) and separation factors (α) for the mentioned cations onto (Pam-Aa) at different radiation dose in 10^{-3} M HNO_3 medium were calculated and tabulated in Table 4. From the data presented in Table 4, it was found that the selectivity order of the investigated cations absorbed on (Pam-Aa) at radiation dose 25 kGy is: $Ni^{2+} > Cd^{2+} > Co^{2+} > Cu^{2+} \geq Pb^{2+} > Zn^{2+}$ while the sequence order of the investigated cations absorbed on (Pam-Aa) at radiation dose 65 kGy is: $Ni^{2+} \approx Cd^{2+} > Cu^{2+} \geq Co^{2+} > Zn^{2+} > Pb^{2+}$ and the selectivity order of the investigated cations absorbed on (Pam-Aa) at radiation dose 90 kGy is: $Co^{2+} > Ni^{2+} \approx Cd^{2+} > Cu^{2+} > Pb^{2+} > Zn^{2+}$. This sequence order supports the sorption of metal ions as unhydrated state except Cd^{2+} ion adsorbed as hydrated state, which may be due to the ionic radii. The ions with smaller ionic radii are easily exchanged and moved faster than that of ions with large ionic radii [29]. The separation factors for the studied cations on (Pam-Aa) at different radiation doses were calculated and indicated that, Ni^{2+} ion has a higher separation factor by 4.56, 2.61, 2.34, 1.33 and 1.18 for Zn^{2+}, Pb^{2+}, Cu^{2+}, Co^{2+} and Cd^{2+} ions, respectively, at radiation dose 25 kGy. While Ni^{2+} ion has a higher separation factor by 2.98, 2.52, 2.24, 1.96 and 1.02 for Pb^{2+}, Zn^{2+}, Co^{2+}, Cu^{2+} and Cd^{2+} ions, respectively, at radiation dose 65 kGy. These values indicated that Ni^{2+} ion can easily separate from hazardous and industrial waste solutions included the abovementioned cations [16]. Co^{2+} ion has a higher separation factor by 4.4, 3.57, 2.75, 1.75 and 1.72 for Zn^{2+}, Pb^{2+}, Cu^{2+}, Cd^{2+} and Ni^{2+} ions, respectively, at radiation dose 90 kGy. These values indicated that Co^{2+} ion can easily separate from radioactive and industrial waste solutions included the abovementioned cations, and reveal that non-selectivity of (Pam-Aa) for Zn^{2+} ion.

The $[H^+]$ dependency of K_d values of Ni^{2+}, Cd^{2+}, Co^{2+}, Pb^{2+}, Zn^{2+} and Cu^{2+} ions onto (Pam-Aa-MgSi) composites prepared at different radiation dose are shown in Figs. 3(e)–(g) and Table 5. The linear relations between $\log K_d$ and $[H^+]$ were observed for Ni^{2+}, Cd^{2+}, Co^{2+}, Pb^{2+}, Zn^{2+} and Cu^{2+} ions with slopes (0.18, 0.3, 0.23, 0.76, 0.7 and 0.18), (0.3, 0.42, 0.45, 0.9, 0.8 and 0.29) and (0.74, 0.5, 0.25, 0.54, 0.64 and 0.52) for (Pam-Aa-MgSi) at radiation doses 25, 65 and 90 kGy, respectively. These slopes are smaller than the valence of the divalent metal ions sorbed, which prove the non-ideality of the exchange reaction. The variation may be due to the prominence of a mechanism other than ion-exchange, such as precipitation, surface adsorption or simultaneous adsorption of anions [6,31].

The distribution coefficients (K_d) and separation factors (α) for the mentioned cations onto (Pam-Aa-MgSi) at different radiation dose in 10^{-3} M HNO_3 medium were calculated and tabulated in Table 5. The data in Table 5 indicate that the distribution coefficients have the sequence order of the investigated cations absorbed on (Pam-Aa-MgSi) at radiation dose 25 kGy is: $Cd^{2+} \geq Zn^{2+} > Pb^{2+} \geq Ni^{2+} > Co^{2+} \approx Cu^{2+}$ while the selectivity order of the investigated cations absorbed on (Pam-Aa-MgSi) at radiation dose 65 kGy is: $Pb^{2+} > Cd^{2+} \approx Co^{2+} > Zn^{2+} \geq Ni^{2+} > Cu^{2+}$ and the selectivity order of the investigated cations absorbed on (Pam-Aa-MgSi) at radiation dose 90 kGy is: $Pb^{2+} > Cd^{2+} > Ni^{2+} > Co^{2+} > Cu^{2+} \geq Zn^{2+}$. This sequence order supports the sorption of metal ions as hydrated state except Zn^{2+} ion adsorbed as unhydrated state, which may be due to the ionic radii. The separation factor for the investigated cations on (Pam-Aa-MgSi) at different radiation doses was calculated and indicated that, Cd^{2+} ion has a higher separation factor by 1.94, 1.93, 1.19, 1.14 and 1.03 for Cu^{2+}, Co^{2+}, Ni^{2+}, Pb^{2+} and Zn^{2+} ions, respectively, at radiation dose 25 kGy. While Pb^{2+} ion has a higher separation factor by 5.45, 3.76, 3.68, 3.33 and 3.33 for Cu^{2+}, Ni^{2+}, Zn^{2+}, Co^{2+} and Cd^{2+} ions, respectively, at radiation dose 65 kGy. And Pb^{2+} ion has a higher separation factor by 2.3, 2.22, 1.62, 1.26 and 1.18 for Zn^{2+}, Cu^{2+}, Co^{2+}, Ni^{2+} and Cd^{2+} ions, respectively, at radiation dose 90 kGy. These values indicated that Pb^{2+} ion can easily separate from radioactive and industrial waste solutions included the abovementioned cations, and reflect non-selectivity of (Pam-Aa-MgSi) for Cu^{2+} ion [16].

References

[1] M. Naushad, S. Vasudevan, G. Sharma, A. Kumar, Z.A. Alothman, Adsorption kinetics, isotherms and thermodynamic studies for Hg^{2+} adsorption from aqueous medium using alizarin red-S-loaded amberlite IRA-400 resin, Desal. Wat. Treat., 57 (2016) 18551–18559.

[2] G. Sharma, B. Thakur, M. Naushad, A.H. Al-Muhtaseb, A. Kumar, M. Sillanpaa, G.T. Mola, Fabrication and characterization of sodium dodecyl sulphate@ironsilicophosphate nanocomposite: ion exchange properties and selectivity for binary metal ions, Mater. Chem. Phys., 193 (2017) 129–139.

[3] A.M. Khan, S.A. Ganai, S.A. Nabi, Synthesis of a crystalline organic inorganic composite exchanger, acrylamide stannic silicomolybdate: binary and quantitative separation of metal ions, Colloids Surf., A, 337 (2009) 141–145.

[4] M. Naushad, Z.A. Alothman, M. Islam, Adsorption of cadmium ion using a new composite cation-exchanger polyaniline Sn(IV) silicate: kinetics, thermodynamic and isotherm studies, Int. J. Environ. Sci. Technol., 10 (2013) 567–578.

[5] Z.A. Alothman, M.M. Alam, M. Naushad, Heavy toxic metal ion exchange kinetics: validation of ion exchange process on composite cation exchanger nylon 6,6 Zr(IV) phosphate, J. Ind. Eng. Chem., 19 (2013) 956–960.

[6] M.M. Abou-Mesalam, M.R. Abass, M.A. Abdel-Wahab, E.S. Zakaria, A.M. Hassan, H.F. Khalil, Complex doping of d-block elements cobalt, nickel and cadmium in magneso-silicate composite and its use in the treatment of aqueous waste, Desal. Wat. Treat., 57 (2016) 25757–25764.

[7] E.A. Abdel-Galil, A.B. Ibrahim, M.M. Abou-Mesalam1, Sorption behavior of some lanthanides on polyacrylamide stannic molybdophosphate as organic-inorganic composite, Int. J. Ind. Chem., 7 (2016) 231–240.

[8] G. Sharma, A. Kumar, M. Naushad, D. Pathania, M. Sillanpaa, Polyacrylamid@Zr(IV) vanadophosphate nanocomposite: ion exchange properties, antibacterial activity, and photocatalytic behavior, J. Ind. Eng. Chem., 33 (2016) 201–208.

[9] A.A. Khan, Inamuddin, M.M. Alam, Preparation, characterization and analytical applications of a new and novel electrically conducting fibrous type polymeric–inorganic composite material: polypyrrole Th(IV) phosphate used as a cation-exchanger and Pb(II) ion-selective membrane electrode, Mater. Res. Bull., 40 (2005) 289–305.
[10] M. Luqman, Ion Exchange Technology I Theory and Materials, King Saud University, Kingdom of Saudi Arabia, 2012.
[11] M.M. Abou-Mesalam, M.A. Hilal, H.A. Arida, Environmental studies on the use of synthesized and natural ion exchange materials in the treatment of drinking and underground water, Arab. J. Nucl. Sci. Appl., 46 (2013) 63–74.
[12] V.J. Inglezakis, S.G. Poulopoulos, Adsorption, Ion Exchange and Catalysis Design of Operations and Environmental Applications, Elsevier, Amsterdam, 2006.
[13] M.M. Abou-Mesalam, I.M. El-Naggar, Selectivity modification by ion memory of magneso-silicate and magnesium alumino-silicate as inorganic sorbents, J. Hazard. Mater., 154 (2008) 168–174.
[14] M. Luqman, Ion exchange technology I: theory and materials, Vol. 1, Springer Science & Business Media, 2012.
[15] Y.K. Lee, J.M. Jeong, B.Y. Yang, Y.S. Lee, B.C. Lee, H. Youn, D.S. Lee, J.K. Chung, M.C. Lee, Nanoparticles modified by encapsulation of ligands with a long alkyl chain to affect multispecific and multimodal imaging, J. Nucl. Med., 53 (2012) 1462–1470.
[16] I.M. El-Naggar, M.M. Abou-Mesalam, Novel inorganic ion exchange materials based on silicates; synthesis, structure and analytical applications of magneso-silicate and magnesium alumino-silicate sorbents, J. Hazard. Mater., 149 (2007) 686–692.
[17] I.M. Ali, Y.H. Kotp, I.M. El-Naggar, Sorption mechanism of some heavy metal ions from aqueous media magnesium silicate, Arab. J. Nucl. Sci. Appl., 43 (2010) 101–113.
[18] I.M. Ali, Y.H. Kotp, I.M. El-Naggar, Thermal stability, structure modifications and ion exchange properties of magnesium silicate, Desalination, 259 (2010) 228–234.
[19] W. Clowutimon, P. Kitchaya, P. Asswasaengrat, Adsorption of free fatty acid from crude palm oil magnesium silicate derived from rice husk, Eng. J., 15 (2011) 15–26.
[20] I.M. Ali, E.S. Zakaria, M.M. Ibrahim, I.M. El-Naggar, Synthesis, structure, dehydration transformations and ion exchange characteristics of iron-silicate with various Si and Fe contents as mixed oxides, Polyhedron, 27 (2008) 429–439.
[21] M.M. Abou-Mesalam, A.S. Amine, M.M. Abdel-Aziz, I.M. El-Naggar, Synthesis and ion exchange characteristic of poly (acrylamide-acrylic acid)-silicon titanate and its use for treatment of industrial waste, Egyptian J. Chem., 46 (2003) 655–670.
[22] M.M. Abou-Mesalam, Retention behavior of nickel, copper, cadmium and zinc ions from aqueous solutions on silico-titanate and silico-antimonate used as inorganic ion exchange materials, J. Radioanal. Nucl. Chem., 252 (2002) 579–583.
[23] M.M. Abou-Mesalam, Structural and crystallographic features of chemically synthesized cero- and titanium cero-antimonates inorganic ion exchangers and its applications, Adv. Chem. Eng. Sci., 1 (2011) 1–6.
[24] A.A. Khan, A.A. Alam, Synthesis, characterization and analytical applications of a new and novel 'organic–inorganic' composite material as a cation exchanger and Cd(II) ion-selective membrane electrode: polyaniline Sn(IV) tungstoarsenate, React. Funct. Polym., 55 (2003) 277–290.
[25] A.A. Khan, Inamuddin, Preparation, physico-chemical characterization, analytical applications and electrical conductivity measurement studies of an 'organic–inorganic' composite cation-exchanger: polyaniline Sn(IV) phosphate, React. Funct. Polym., 66 (2006) 1649–1663.
[26] M.M. Abou-Mesalam, M.R. Abass, A.B. Ibrahim, E.S. Zakaria A.M. Hassan, Polymeric composite materials based on silicate: I-synthesis, characterization and formation mechanism, Int. J. Innovative Res. Growth, 6 (2018) 66–82.
[27] S.A. Nabi, S. Usmani, N. Rahman, Synthesis, characterization and analytical applications of an ion exchange material: zirconium (IV) iodophosphate, In Annales de Chimie, 21 (1996) 521–530.
[28] S.A. Shady, Selectivity of cesium from fission radionuclides using resorcinol formaldehyde and zirconyl-molybdopyrophosphate as ion exchangers, J. Hazard. Mater., 167 (2009) 947–952.
[29] I.M. El-Naggar, E.A. Mowafy, E.A. Abdel-Galil, M.F. El-Shahat, Synthesis, characterization and ion-exchange properties of a novel 'organic-inorganic' hybrid cation-exchanger: polyacrylamide Sn(IV) molybdophosphate, Global J. Phys. Chem., 1 (2010) 91–106.
[30] R. Bushra, M. Naushad, G. Sharma, A. Azam, Z.A. Alothman, Synthesis of polyaniline based composite material and its analytical applications for the removal of highly toxic Hg^{2+} metal ion: antibacterial activity against *E. coli*, Korean J. Chem. Eng., 34 (2017) 1970–1979.
[31] Y.F. El-Aryan, E.A. Abdel-Galil, G.E. Sharaf El-deen, Synthesis, characterization, and adsorption behavior of cesium, cobalt, and europium on polyacrylonitrile titanium tungstophosphate organic-inorganic hybrid exchanger, Russ. J. Appl. Chem., 88 (2015) 516–523.